Article ID: 1000-9116(2006)05-0569-12

Development and application of the moment-ratio imaging algorithm*

HUANG Jian-ping[1,2),♣] (黄建平) MA Li[1)] (马 丽) ZHANG Chao-jun[1,2)] (张晁军)

1) *Institute of Earthquake Sciences*, *China Earthquake Administration*, *Beijing* 100036, *China*
2) *Graduate University of Chinese Academy of Sciences*, *Beijing* 100049, *China*

Abstract

In the moment-ratio imaging algorithm, which is based on the theory of healing of a wound, the energy of each strong earthquake is distributed around the epicenter according to certain rules, and the features of the Moment-ratio value $\mathcal{M}$ are analyzed as the space and time change, so that the relationships between the moment-ration value $\mathcal{M}$ and strong earthquakes can be found. In the present paper, regions divided, hypocenter depths and events completed magnitude analyses were carried out in the Chinese catalogue. By applying the moment-ratio imaging algorithm in which the parameters are adjusted, the processes of anomaly evolution which correspond to the epicenter and the surrounding value $\mathcal{M}$ before earthquakes of $M\geq 7.0$ since 1966 in different areas of China were analyzed. It was found that the range area and imminent time of a coming earthquake could be confirmed quantitatively by analyzing the abnormal temporal and spatial variation of the value $\mathcal{M}$. The results showed that the temporal and spatial variation of the value $\mathcal{M}$ could quantitatively reflect the temporal and spatial factors of a coming strong earthquake as well as the rule of medium rupture.

Key words: **moment-ratio imaging algorithm**; **healing, quantitative analysis**; **China strong earthquakes**
CLC number: P315.75 **Document code**: A

Introduction

After an earthquake occurs, the regional stress field will be adjusted, the stress state in the epicenter area is relatively weak and the loaded stress at the crustal medium in the surrounding area will relatively increase due to the energy release of the crustal rupture. When several small and medium earthquakes occur, one or several new stress-concentrated areas will appear due to the effect of every event. The comprehensive effect could be related to the time, space and magnitude of every coming event and it is the parameter function of every event. Therefore, the coming event will be the result of the comprehensive effect (Department of Earthquake Monitoring and Prediction, China Earthquake Administration, 2002). This point of view takes the effect of already-happened earthquakes on the regional stress field as the ″cause″ of a strong earthquake, from which angle many prediction methods based on different physical models are brought out.

Since Fedotov (1965) defined the seismic gap in 1965, the concept of gap has been a focused zone in long-term prediction of studying future risk region for a long time and its form has been

* **Received** 2005-11-23; **accepted in revised form** 2006-06-12.
Foundation item: National Natural Science Foundation of China (40574020 and 10371012).
♣ **Author for correspondence**: huangjianping@seis.ac.cn

developing all the time (Mogi, 1979; LU *et al*, 1982, 1983; Nishenko, 1985; HAN *et al*, 1989; Wyss and Wiemer, 1999). WANG *et al* used one systematic indicator for the abnormal stage estimation such as seismic dangerous degree *D*-value (WANG and LIU, 1987), seismic magnitude factor *Mf* value (WANG *et al*, 1994), seismic spatial concentrative degree *C* value (WANG *et al*, 1999a), seismicity factor *A* value (WANG *et al*, 1999b), and used them for the medium-term and short-term earthquake prediction.

YIN and YIN (1991), YIN *et al* (1994) put forward the theory of LURR (Loading and unloading response ratio), the *Y* value of which can describe the earthquake development. The *Y* value can quantitatively measure the progress of the earthquake development in a certain area medium, thus, it is possible to use it for earthquake forecasting. While in the algorithm of *M*8 advanced by Russian, seven functions are used to describe various seismicity before strong earthquakes ($M>8$) and to search the time increase probability (TIP) (Keilis-Borok and Kossabokov, 1990; MA and Vere-Jone, 1997). As to the reverse tracing of precursors method, eight functions are adopted to depict the seismicity so as to determine the possibility of the next strong earthquake (Keilis-Borok *et al*, 2004).

Lomnitz (1985) analyzed the relationship between the epicenters and rupture directions of successive earthquakes ($M\geq7.0$) in Chile and Mexico, and advanced the concept of healing to explain such phenomena founded on the energy exchange and mantle convection. Then the moment ratio imaging (MRI) algorithm was developed (Lomnitz, 1993, 1994, 1996a). With the algorithm, the normalized residual moment was calculated, and the variations of value $\mathcal{R}$ prior to strong earthquakes were compared in the areas of Chile, Mexico and Japan. It was found that with the appearance of high values $\mathcal{R}$ the strong earthquakes would occur in certain regions.

In the present paper, the MRI algorithm is adopted to analyze the earthquakes ($M\geq7.0$) since 1966 in China, so as to look for methods of suitable parameters within China from different points of view, and to analyze the features of the spatial and temporal variation of the value $\mathcal{R}$ prior to strong earthquakes.

1 Algorithm of moment ratio imaging

1.1 Basic theory

Suppose that an earthquake of seismic moment M_0 occurs at $t=0$. Since M_0 equals the displacement times the area of rupture and since we lack direct measurements of either, the best way is to replace the area of rupture with M_0 equally. Let us call this area a scar. Now as the scar heals, its size decreases exponentially with time:

$$m_0(t) = M_0 \exp(-0.69315 \times t / \tau) \tag{1}$$

where M_0 is the initial seismic moment, namely, the initial size of the scar. The constant −0.693 15 is ln(1/2), when $t=\tau$, $m_0=M_0/2$, such a constant can be got. τ is the half-life of the seismic moment M_0, which is the last time when m_0 equals half of M_0. m_0 is called the residual moment t years after the event.

Equation (1) describes the healing process of a single event. However, an event does not happen individually, it occurs under the effect of the inner structural system and that between the tectonic blocks. At the same time, the occurrence of an event will definitely affect the surrounding area. The way of expressing such an effect is to distribute the moment M_0 within one region

around the epicenter according to a certain rule.

Furthermore, by assuming the rupture process as a linear overlap of moment anomalies in space and time, we may generalize this result for continuous plate boundaries, that is

$$m_0(t) = M_0 \exp(\frac{-0.69315 \times t}{\tau}) + \sum_{j=1}^{i} M_{0j} \exp\left[\frac{-0.69315 \times (t - t_j)}{\tau}\right] \tag{2}$$

where M_{01}, M_{02},……, M_{0j} are the major earthquakes in the segment during the preceding time interval [0, t].

When an earthquake occurs, its moment M_0 is accumulated. Then it is multiplied by $\exp(-0.69315 \times \Delta t)$ iteratively for every time step Δt. Carry out the same procedure for each region, then we obtained graphs of the residual moment m_0 along a plate boundary.

In order to compare the healing process between regions with different levels of earthquake activity, a more practical way of imaging residual moment is to calculate the normalized moment

$$\Re = \frac{M_{0\text{tot}}}{\sum_{t=t_0}^{t_{\text{end}}} m_0(t)} \tag{3}$$

The nondimensional value $\Re$ is called the moment ratio. Here $M_{0\text{tot}}$ is the total accumulated seismic moment released by the region over the time spanned by the catalogue. The sum in the denominator, which is calculated by equation (2), is the residual seismic moment in the region up to time t_{end}. Thus, the value $\Re$ is the reciprocal of the normalized residual moment. The purpose for doing this is to turn every bounded trough in m_0 into an unbounded peak in $\Re$. The procedure of graphing $\Re$ variation with time in different regions is called moment ratio imaging (MRI) (Lomnitz, 1994).

1.2 Half-life time of seismic moment anomaly

One of the main problems is how to set the parameter τ in equation (1) when MRI algorithm is applied to studying the characteristics of seismic gaps preceding strong earthquakes in China. Lomnitz (1985) studied the relationship among the time, length and direction of the ruptures in 8 earthquakes (M>7.0) since 1822 in Chile (Figure 1), and found that rupture length would decay exponentially with time, so he set 20 years for τ in the region.

When Lomnitz (1994) studied the relationship of the locations among all earthquakes, one can see from Figure 1 that the rupture directions are based on

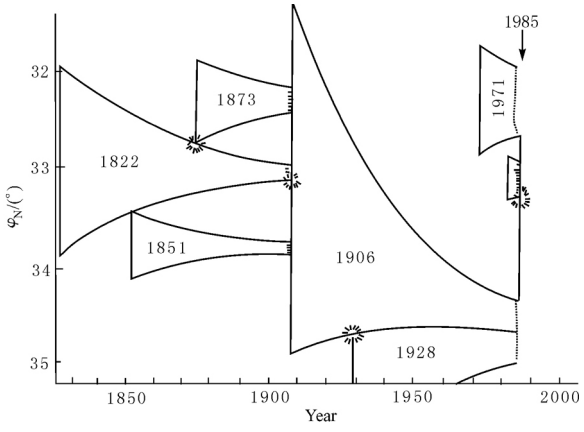

Figure 1 The attenuation process of seismic rupture (Lomnitz, 1994)

The stars stand for the latitudes of the earthquakes, the numbers stand for the year of the earthquake occurrences, the bars stand for the initial rupture length of the earthquakes, and the curves describe the healing process of the ruptures exponential attenuation

the latitude direction, which is very convenient in the regions surrounding the Pacific Ocean. The reason is that the rupture directions in these regions are usually along the direction of longitudes, so the location of the epicenter; the rupture length and the rupture direction of each earthquake in the regions can be compared directly to decide the parameter τ. While in the regions selected in the paper, the rupture directions of earthquakes vary to a great extent, so this method is unsuitable. Since the physical meaning of half-life time is the last time when m_0 equals half of M_0, and the earthquake repeat period is the last time of seismic moment complete attenuation, there would be a certain ratio relationship between the half-life time τ and the repeated period. Thus, the Gutenberg-Richard magnitude-frequency relationship (G-R) is used to calculate the repeat period T_M (LIU, 2004; Schorlemmer and Wiemer, 2004) in the paper. According to the value T_M, different ratios α are selected, and by equation (4)

$$\tau = T_M \times \alpha \tag{4}$$

the half-life time τ of different magnitude will be got and put into MRI algorithm. The main reason to select different ratios α is that the quantitative relationship between the repeat period T_M and the half-life time τ is unknown.

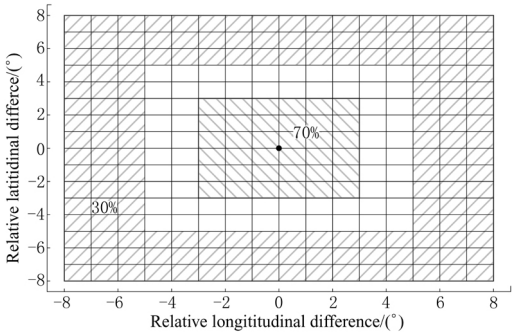

Figure 2 Sketch of energy distribution of Mexico Hat model
70% of the moment is distributed in the distance 0°~3° (135° backlash area), each grid is 1/36; no moment is distributed in the distance 3°~5° (blank area); 30% of the moment is distributed in the distance 5°~8° (45° slash area), each grid is 1/156

1.3 Scheme of energy distribution

Besides the problem of setting the values of τ when MRI algorithm is used, another problem is to set the scheme of energy distribution, that is, how to distribute the seismic energy in space. Based on the analysis of spatial distances of successive earthquakes (M≥7.0) from January 1, 1900 to December 31, 1989 around the globe, Lomnitz (1996b) found that the distance variation between two successive earthquakes follows the rule of spherical Bessel function. Combined with aftershock pattern, Lomnitz advanced the ″Mexican Hat″ model and explained it from the physical mechanism perspective. The scheme of energy distribution is shown in Figure 2.

However, it seems abhorrent to the theory of seismic wave propagation if the middle gap section is distributed without energy. It is hard to understand that energy propagation will jump the gap section and only leave behind the energy at two ends. Furthermore, the degree 8 is got according to the global catalogue. Is it suitable for Chinese mainland? And what is the way of energy distribution with magnitude between 5.0 and 6.9? Here the Chinese catalogue from January 1, 1900 to December 31, 2004 with magnitude of more than 5.0 is selected, and the spatial distance frequencies of successive earthquakes are studied, so as to decide the way of energy distribution within different magnitude span.

2 Data and its management

The seismic catalogues used here include two parts. The Chinese mainland catalogue covers a span from the time when there is record to the end of 2004, in which the catalogue from the 23th

century BC to 1911 is taken from ″Historical Strong Earthquakes in China″ (Department of Disaster Prevention, State Seismological Bureau, 1995), and the catalogue from 1912 to 1990 is taken from ″China Modern Earthquakes Catalogue″ (Department of Disaster Prevention, China Seismological Bureau, 1999). The catalogue after 1991 is taken from the C01 files in Chinese Earthquake Network Center, China Earthquake Administration. The Taiwan Catalogue is from Statistical Seismological Library[①] (SSLib), which covers the time span from January 1, 1900 to December 31, 2003.

According to the catalogues above, the management in this paper includes the following three parts (HUANG *et al*, 2005):

1) Sub-regions selection. According to the seismic regions divided within China by LI (2003), together with the locations of epicenter (M≥7.0) in ″Earthquake Cases in China″ (ZHANG, 1988, 1990; CHEN, 2002a, b), North China, Northwest China, Southwest China and Taiwan are selected as the study subject.

2) Depth of shallow events selection. In Table 1, the information regarding all the target events is listed. Only shallow earthquakes are selected and analyzed. Firstly, three analyses are carried out in the paper: ① On a certain fixed depth segment, the frequencies of events are analyzed with difference magnitude scales in order to look for the magnitude scale which can reflect the depth change; ② on a certain fixed magnitude scale, the frequencies of earthquakes are analyzed with difference depth segments; ③ All the events are projected along the vertical direction of the major tectonic structure zones within one region, and the plots of depth profile can be obtained. Then by combining these analyses, the depth range of shallow earthquakes can be set within different regions.

Table 1 The information of studied earthquakes

No.	Sub region	Earthquake	Date a-mo-d	φ_N/(°)	λ_E/(°)	M	Depth/km	Remark
1	NC	Xingtai	1966-03-22	37.5	115.1	7.2	9	E
2	NC	Bohai	1969-07-18	38.2	119.4	7.4	35	E
3	SW	Tonghai	1970-01-05	24.1	102.6	7.7	13	**E**
4	SW	Luhuo	1973-02-06	31.5	100.4	7.7	17	E
5	SW	Daguan	1974-05-11	28.2	104.1	7.1	10	E
6	NC	Haicheng	1975-02-04	40.65	122.8	7.3	12	E
7	SW	Longling	1976-05-29	39.56	118.0	7.8	11	E
8	NC	Tangshan	1976-07-28	39.56	118.0	7.8	11	E
9	SW	Songpan	1976-08-16	32.5	104.3	7.2	23	E
10	Taiwan	Taiwan Strait	1994-09-16	22.5	118.73	7.2	19	E
11	SW	Menglian West	1995-07-12	22.04	99.20	7.2	13	E
12	Taiwan	Chichi	1999-09-20	23.85	120.81	7.3	8	SSLib
13	NW	Kunlun Mountain West	2001-11-14	35.93	90.53	8.1	10	C

Note: In the column of sub-region, NC stands for North China, NW for Northwest China, SW for Southwest China; in the column of remark, E stands for earthquake cases in China, C for China Earthquake Net Center.

3) Complete magnitude selection. Within different periods, the density and the record accuracy of seismic stations are different. According to previous research results (Gutenberg and Richter, 1944, 1954; Ustu, 1990), within some space and time period, the frequencies of all earthquakes satisfy the relation of G-R, but actually the deviation of events from the fit-line in the loga-

① Harte D S. 1998. Documentation for the statistical seismology library. School of Mathematical and Computing, Sciences Research Report, 93~98.

rithm of frequency and magnitude plot is always great for events with small and large values of magnitude. This phenomenon is generalized as the incompleteness of records (CHEH *et al*, 2003; CHEN *et al*, 2002; WANG *et al*, 2004). In the present paper, the deviation point of the G-R relation for small events was searched in order to set the magnitude cutoff M_c in each time segment. The sketch of the fitting method is shown in Figure 3. In the plot of the G-R relation, started from the minimum magnitude M_0, a group of data with the percentile of 5%~15% and another group of data with the percentile of 25%~75% (the percentiles can be moving adjusted) are selected to fit two lines respectively, then the crossing point of the two lines is considered as the magnitude cutoff M_c. In the paper, the catalogue is divided by equal numbers of the events to get the M_c in each time period, and together with the yearly frequency with events of M≥5.0, their starting time can be confirmed.

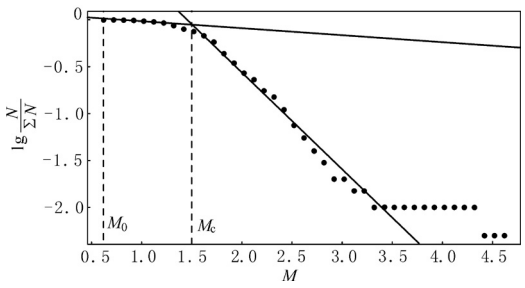

Figure 3 Sketch of fitting G-R relation to search the deviation point for small event

Based on the management of the three parts above, the catalogues with M≥5.0 are obtained in each region (Table 2). For the time periods and depth ranges are the same in the east and west regions in Taiwan, the two regions are united into one in the parameter analysis of MRI.

Table 2 Selected earthquakes with M≥5.0 in each region

Sub-region	Time span a-mo-d	Depth/km	Number of earthquakes
North China	1480-01-01~2004-12-31	0~35	333
Northwest China	1900-01-01~2004-12-31	0~40	504
Southwest China	1900-010-1~2004-12-31	0~35	771
Taiwan	1900-01-01~2003-12-31	0~40	631

3 Calculation results and analysis

3.1 Parameters decision

Applying different α into equation (4), then the values τ of different magnitudes are got. Here α is 0.01, 0.02, ⋯, 0.1, 0.2, ⋯⋯ and 1.0. The rule to get the best α is that the value $\mathcal{R}$ at the epicenter minus the value $\mathcal{R}$ around the epicenter and the difference should be more than 0.5, so as to easily visualize the high value at the epicenter. The results show that the best α is 0.1.

The ratios k_i is the number of events in the ith region divided by the total number of the events in all regions, and it is calculated by equation (5)

$$k_i = \frac{N_i}{\sum_{i=1}^{j} N_i} \tag{5}$$

Where N_i is the number of events within ith degree distance to the epicenter in the magnitude scale shown in Table 3, and k_i is the ratio for ith degree. For different magnitude scales, the value j depends on the statistical relation between magnitudes and rupture lengths (ZHANG *et al*, 2001).

The results are listed in Table 3.

Table 3 Ratios of energy distribution within different distances

Magnitude scale	Distance to epicenter/(°)						
	1	2	3	4	5	6	7
5.0~5.3	1.00	0	0	0	0	0	0
5.4~5.8	0.854	0.146	0	0	0	0	0
5.9~6.4	0.72	0.118	0.162	0	0	0	0
6.5~6.8	0.78	0.06	0.100	0.05	0.01	0	0
≥6.5	0.647	0.163	0.02	0.036	0.043	0.041	0.049

As is seen in Table 3, the maximum distance varies with different magnitude scales. Even within the same magnitude, the ratio varies with the epicenter distance. By applying these parameters into the equation (3), the image of value $\mathscr{R}$ preceding each target earthquake can be got.

3.2 Characteristics of value $\mathscr{R}$

Among the 13 study cases, the variation characteristics of value $\mathscr{R}$ in 12 events are compatible, that is to say, started from a certain time preceding the target earthquake (Table 4), the value $\mathscr{R}$ in the future epicenter is relatively and abnormally high than that in the surrounding area. If no other strong earthquake occurs in the surrounding area, then the abnormal range will increase continually until the event comes. Otherwise, the range of value $\mathscr{R}$ near and in the epicenter will decrease due to the effect of the surrounding strong earthquakes, but in the future epicenter area the value $\mathscr{R}$ is still relatively high. After the target earthquake, the high abnormal value $\mathscr{R}$ will disappear in the epicenter and surrounding area, and the value $\mathscr{R}$ will turn low in the epicenter. While in Longling earthquake in Yunnan Province, the value $\mathscr{R}$ preceding the event increased continually, but it did not decrease after the event and remained relatively high.

Based on the analysis of the studied cases, the average warning values of $\mathscr{R}$ are found (Table 4). When the value $\mathscr{R}$ is larger than the warning value, the region will be in risk duration. The risk is dependent on the value $\mathscr{R}$ in one region, namely, the higher the value $\mathscr{R}$ is, the more possible that there will be a strong earthquake, and the shorter it is before the strong earthquake occurs. As is seen in Table 4, except the smaller warning value $\mathscr{R}$ in North China, the warning values $\mathscr{R}$ are almost the same in the other three regions, which is in accordance with the regional seismicity.

Table 4 Characteristics of $\mathscr{R}$ values in studied regions

Regions	Duration of the value $\mathscr{R}$/a	Maximum of value $\mathscr{R}$	Averages warning value $\mathscr{R}$
North China	20~25	5.8	3.5
Northwest China	15~20	6.9	3.9
Southwest China	15~20	7.2	4.0
Taiwan	15~20	6.6	4.0

3.3 Features of value $\mathscr{R}$ before and after strong earthquakes

Tangshan earthquake on July 28, 1976 was researched as an example in North China, in order to illustrate the features of the spatial and temporal variation of the value $\mathscr{R}$ (Figure 4).

As is seen in Figure 4, the value $\mathcal{R}$ in the epicenter area of Tangshan (7: x-axis in Figure 4) was relatively high and continued rising preceding Xingtai earthquake in 1966. After 1966, the value $\mathcal{R}$ dropped in the epicenter area of Tangshan whenever a strong earthquake of M≥7.0 occurred, including Xingtai, Bohai Sea and Haicheng events, but it was still relatively high. Besides, the variation characteristics of the value $\mathcal{R}$ in the epicenter before and after Bohai Sea earthquake can also be seen in Figure 4: The value $\mathcal{R}$ increased continuously before Bohai Sea event, and the previous event within the distance of 7 degrees (Xingtai event) would decrease the value $\mathcal{R}$ in the area, thus the value $\mathcal{R}$ dropped to a trough after Bohai Sea event.

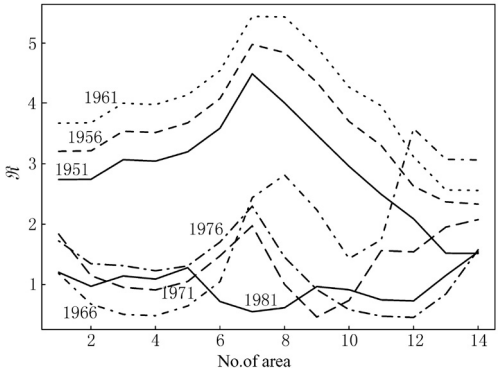

Figure 4 The spatial and temporal variations of the value $\mathcal{R}$ shown in the area of 7 degrees along the west and east of the latitude direction round Tangshan earthquake (28 July 1976) epicenter
α=0.1, and the low magnitude is 5.0. The horizontal axis is the location coding along the latitude direction of the epicenter. The figure shows 14 cells in the area of 7 degrees along the east and west direction of epicenter, and the Xingtai earthquake, Tangshan earthquake, Bohai Sea earthquake and Haicheng earthquake occurred in the cell of 4, 7, 9, and 12 respectively. Each line is the year of the ending for the value $\mathcal{R}$, which is the year of 1951, 1956, 1961, 1966, 1971, 1976, and 1981 respectively

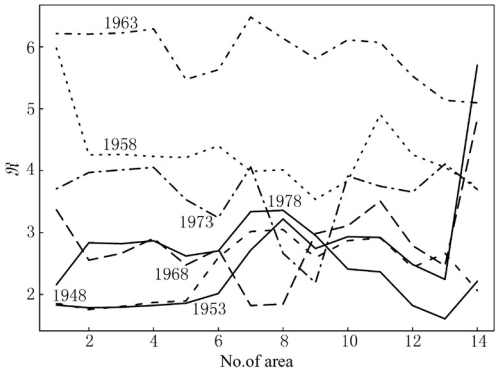

Figure 5 The spatial and temporal variations of the value $\mathcal{R}$ shown in the area of 7 degrees along the west and east of the latitude direction of Luhuo earthquake (February 6, 1976) epicenter
α=0.1, and the low magnitude is 5.0. The horizontal axis is the location coding along latitude direction of the epicenter. The figure shows 14 cells in the area of 7 degrees along the east and west direction of epicenter. Each line is the year of the ending for the value $\mathcal{R}$, which is the year of 1948, 1953, 1958, 1963, 1968, 1973, and 1978 respectively

The variation of the value $\mathcal{R}$ in the epicenter and the surrounding area before and after Luhuo, Sichuan earthquake on February 6, 1973 is shown in Figure 5. It can also be seen that the value $\mathcal{R}$ in the epicenter area increased (from 1948 to 1963). The significant drop of the value $\mathcal{R}$ in the epicenter area in 1968 was the effect of an earthquake (M=7.0) occurred in the northwest region of the epicenter area on April 19, 1963. Later on, the value $\mathcal{R}$ kept rising, then it decreased after Luhuo event. Although the value $\mathcal{R}$ in the epicenter area did not drop to a trough after the event as that of Tangshan event, it was already below the average warning value, which followed the general rule of variation.

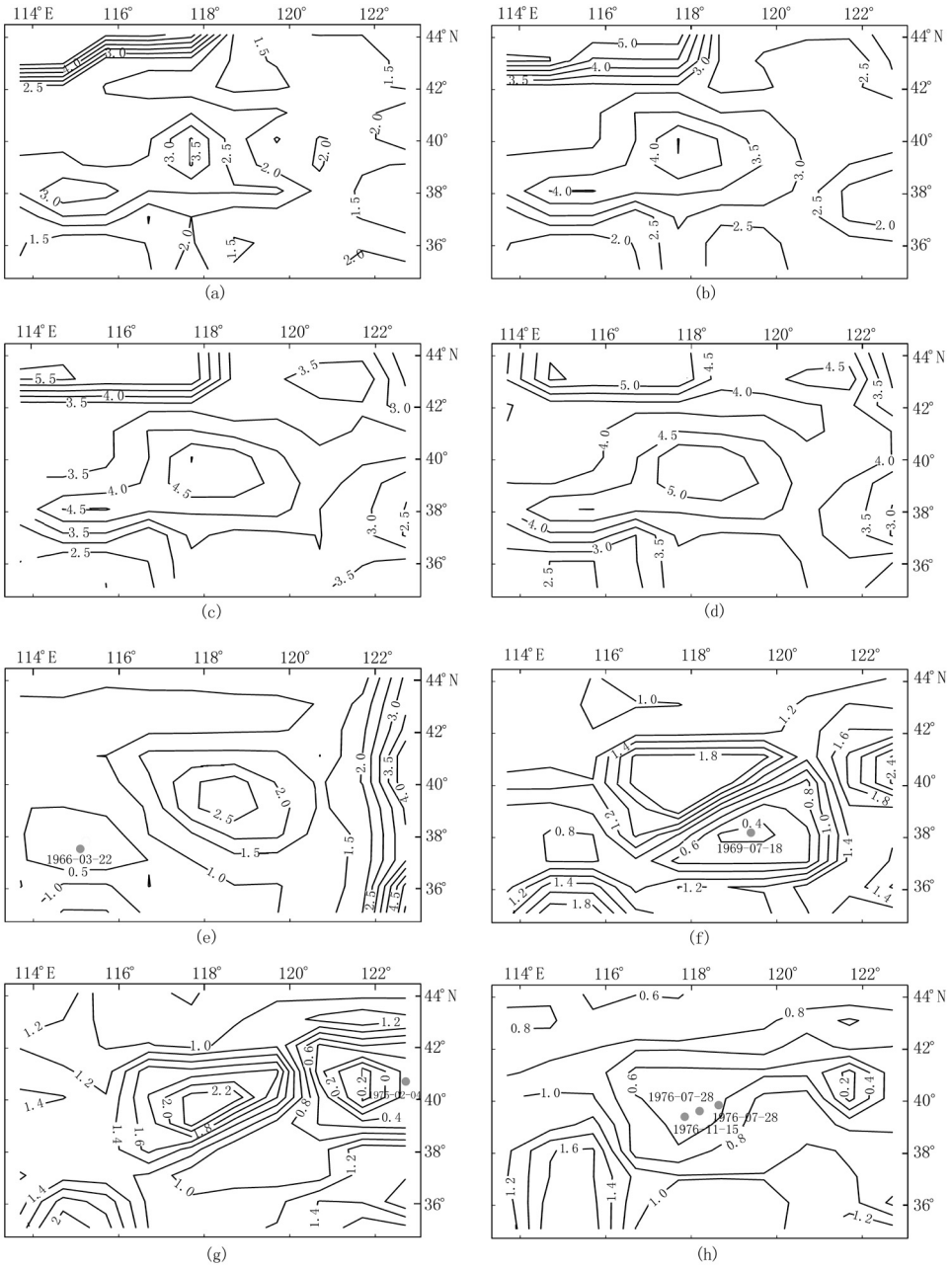

Figure 6 The spatial and temporal variations of the value $\mathcal{R}$ shown in the area of 7 degrees along the west and east of the latitude direction round Tangshan earthquake (February 6, 1976) epicenter

α=0.1, and the low magnitude is 5.0. The epicenter of Tangshan earthquake is located on 39.56°N, 118.0°E. The gray circles present the epicenter of earthquakes ($M\geq7.0$) during different time period, and the numbers show the dates of earthquakes. (a) 1942 1946; (b) 1947 1951; (c) 1952 1956; (d) 1957 1961; (e) 1962 1966; (f) 1967 1971; (g) 1972 1976; (h) 1977 1981

In order to present more clearly the spatial variation of the value $\mathcal{R}$ before and after Tangshan earthquake, the contour of the value $\mathcal{R}$ in the area of Tangshan earthquake was shown in Figure 6.

As is seen in Figure 6, 30 years before Tangshan earthquake, there was a relative anomaly of the value $\mathcal{R}$ around the epicenter in the figure of 1946 (Figure 6a). Moreover, there was a peak in the southwest part, which corresponded to the location of the epicenter area in Xingtai earthquake. Till 1951 (Figure 6b), the two abnormal regions were united into one abnormal area, and the maximum of the value $\mathcal{R}$ was in Tangshan area. At this time, the abnormal area was obviously larger than that in 1946, extending from 0.5 to 3 degrees, and the value $\mathcal{R}$ arose from 3.4 to 4.5. In the next 10 years, the space range of the abnormal value $\mathcal{R}$ further extended (Figure 6c and 6d)), and the significance of the abnormal value $\mathcal{R}$ enhanced. After Bohai Sea and Xingtai event occurred one after another, the value $\mathcal{R}$ decreased from above 3.0 to below 3.0 in the whole area. Especially in the epicenter of Xingtai event, the value $\mathcal{R}$ dropped from 4.1 down to 0.6, while there was no significant difference between the value $\mathcal{R}$ in the areas of Tangshan, Xingtai, Bohai Sea and Haicheng (Figure 6e and 6f)). After Haicheng earthquake, there was an obvious abnormal value $\mathcal{R}$ in the epicenter of Tangshan (Figure 6g), the range of which was lower than the value in patterns of 1946~1961, and the high value $\mathcal{R}$ covered about 4 degrees, that is 2 degrees around Tangshan area. Finally after the Tangshan earthquake, the high value $\mathcal{R}$ area disappeared (Figure 6h).

According to the analysis of Figure 4 and 5, the regional high abnormal value $\mathcal{R}$ could reflect the seismic risk. A good relationship was reflected between Tangshan earthquake and the variations of the value $\mathcal{R}$ calculated by MRI algorithm.

4 Discussion and conclusions

In the present paper, the methods to calculate and adjust parameters were advanced based on the MRI algorithm. The variation characteristics of the value $\mathcal{R}$ before and after the earthquake were studied in the epicenter and surrounding area of 13 earthquakes, and the quantitative relationship was obtained between the variation tendency of the value $\mathcal{R}$ and the future regional earthquake, that is, when the regional value $\mathcal{R}$ exceeded the warning value $\mathcal{R}$, a strong earthquake would occur. The regional warning values $\mathcal{R}$ were different in different regions. Furthermore, when there is a strong earthquake occurrence in surrounding area, the regional warning value $\mathcal{R}$ will be affected and drop.

The characteristics of temporal variation of the value $\mathcal{R}$ in the same region were also shown in the results. Such variation characteristics were consistent with the medium rupture processes, that is, when there is no strong earthquake in surrounding area, the value $\mathcal{R}$ will increase gradually, which means that the seismic risk rises gradually. This reflects the regional energy or stress-accumulated process. When the accumulated energy was up to some extent, the regional value $\mathcal{R}$ also reached to the warning level. When a strong earthquake occurred in surrounding area, the stress field was readjusted due to the released stress, which made the value $\mathcal{R}$ drop. But at this time the medium was broken through the original rupture level, so it would be ruptured by rela-

tively small energy. Therefore, even though the value $\mathcal{R}$ was small, there would still be a strong earthquake.

The methods of parameters calculation here are based on a certain physical meaning, so it is important for the methods of parameters calculation. According to the features of seismicity in China, Lomintz′s method (1993, 1994, 1996a) was not used to determine the half-life τ. Instead, the calculation method of parameter τ was based on the concept of earthquake cycle and the adjustment of the parameter α, so as to get the τ for best accordance with the factual seismicity.

For the scheme of energy distribution, Lomnitz′s idea (1993, 1994, 1996b) was used for reference and a smoothing analysis was done further. In this paper, the relationship between the long axis of background gap and magnitude, rupture length and magnitude, and concept of the earthquake triggering, *etc*. were considered, the disadvantage in Mexico Hat model where there is a gap without any energy was supplemented, which made it better accord with the seismicity features in China. As is seen in Figure 4, the value $\mathcal{R}$ in the epicenter area in Tangshan was affected by several earthquakes preceding Tangshan event, but such effect was conditioned by distance. That is why different weight factors were set in different distances for the energy distribution.

There are still some issues for further research in the MRI algorithm. For example, the medium is considered symmetrical and simplex. How is the energy redistributed quantitatively according to tectonic features in different directions? These are some jobs for further study.

Acknowledgements We are grateful to Cinna Lomnitz for his constructive suggestion and LI Yong, CHEN Shi-jun, DANG Sheng-jun, WANG Li-ping, LIU Wen-bing, YIN Bao-jun, Ray Brownrigg for their help.

References

CHEN Pei-shan, BAI Tong-xia, LI Bao-kun. 2003. *b*-value and earthquake occurrence period [J]. *Chinese J Geophys*, **46**(4): 510~519 (in Chinese).

CHEN Qi-fu. 2002a. Earthquake Cases in China (1992~1994) [M]. Beijing: Seismological Press, 358~390 (in Chinese).

CHEN Qi-fu. 2002b. Earthquake Cases in China (1995~1996) [M]. Beijing: Seismological Press, 97~145 (in Chinese).

CHEN Shi-jun, WANG Li-feng, MA Li, *et al*. 2002. Arguments on the magnitude-frequency relation [J]. *Acta Seismologica Sinica*, **15**(2): 187~197.

Department of Disaster Prevention, China Seismological Bureau. 1999. *Earthquake Catalogues in Modern China* (1912~1990) [M]. Beijing: China Science and Technology Press, 1~633 (in Chinese).

Department of Disaster Prevention, State Seismological Bureau. 1995. Historical strong earthquakes in China [M]. Beijing: Seismological Press, 1~512 (in Chinese).

Department of Earthquake Monitoring and Prediction, China Earthquake Administration. 2002. *Methods and Their Application of Mid- and Imminent Prediction for Strong Earthquakes* [M]. Beijing: Seismological Press, 315~356 (in Chinese).

Fedotov S A. 1965.（Regularities of the distribution of strong earthquakes in Kamchatka, the Kuril Islands and northeast Japan [J]. Trudy Inst Fiz Zemli, *Acad Nauk, SSSR*, 36(203), 66~93 (in Russian).

Gutenberg B and Richter C F. 1944. Frequency of earthquakes in California [J]. *BSSA*, **34**: 181~188.

Gutenberg B and Richter C F. 1954. *Seismicity of the Earth and the Associated Phenomena* [M]. Princeton: Princeton University Press, 1~38.

H AN Wei-bin, JIANG Dao-chong, YANG Hong, *et al*. 1989. Study of gaps in Sichuan Province based on the *R-t*, *D-t* and epicenter figures [A]. In: XU Shao-xie, LU Yuan-zhong, ZHU Chuan-zhen, *et al* ed. *Search Corpus of Earthquake Forecast Applied Method* (*Special of Seismology*) [C]. Beijing: Academic Press, 25~40 (in Chinese with English abstract).

HUANG Jian-ping., MA Li, CHEN Shi-jun, *et al*. 2005. Quantificational analysis to the characterristics of seismicity and quiescence. *Earthquake Research in China*, **21**(3): 417~428 (in Chinese with English abstract).

Keilis-Borok V I and Kossobokov V G.. 1990. Premonitory activation of seismic flow: Algorithm M8 [J]. *Phys Earth Planet Inter*, **61**: 73~83.

Keilis-Borok V, Shebalin P, Gabrielov A, *et al*. 2004. Reverse tracing of short-term earthquake precursors [J]. *Phys Earth Planet Inter*, **145**: 75~85.

LI Xiang-gen. 2003. *Panorama of the Neo-tectonics Movement in China* [M]. Beijing: Seismological Press, 253~564 (in Chinese).

Liu Zheng-rong. 2004. *Methods of Earthquake Prediction* [M]. Beijing: Seismological Press, 42~53 (in Chinese).

Lomnitz C. 1985. Tectonic feedback and earthquake cycle [J]. *Pure Appl Geophys*, **123**: 667~682.

Lomnitz C. 1993. Moment-ratio imaging of seismic regions for earthquakes prediction [J]. *Geophys Res Lett*, **20**(20): 2 171~2 174.

Lomnitz C. 1994. Fundamental of Earthquake Prediction [M]. New York: John Wiley & Sons Inc., 88~127.

Lomnitz C. 1996a. Predicting earthquakes with the MRI algorithm [J]. *Seism Res Lett*, **67**(6): 40~46.

Lomnitz C. 1996b. Search of a Worldwide Catalogue for Earthquakes Triggered at Inter- mediate Distances [J]. *Bull Seism Soc Amer*, **86**(2): 293~298.

LU Yuan-zhong, SHEN Jian-wen, SONG Jun-gao. 1982. Seismic gap and approaching earthquake [J]. *Acta Seismologica Sinica*, **4**(4): 327~336 (in Chinese with English abstract).

LU Yuan-zhong, WANG Wei, SHEN Jian-wen. 1983. Seismic gap and approaching earthquake (continued) [J]. *Acta Seismologica Sinica*, **5**(2): 129~144 (in Chinese with English abstract).

MA Li and Vere-Jones D. 1997. Application of *M*8 and Lin-Lin algorithms to New Zealand earthquake data. New Zealand [J]. *Journal of Geology and Geophysics*, **40**: 77~89.

Mogi K. 1979. Two kinds of seismic gaps [J]. *Pure Appl Geophys*, **117**: 1 172~1 186.

Nishenko S P. 1985. Seismic potential for large and great interplate earthquakes along the Chilean and southern Peruvian margins of South America: a quantitative reappraisal [J]. *J Geophys Res*, **90**(B5): 3 589~3 615.

Schorlemmer D and Wiemer S. 2004. Earthquake statistics at Parkfield: 1 Stationary of *b* values [J]. *J Geophys Res*, **109**(B12307), 1~17.

Ustu. LI Yu-che, LU Zhen-ye, DING Jian-hai trans. 1990. *Earthquake*? [M]. Beijing: Seismological Press. 212~215 (in Chinese).

WANG Li-feng, MA Li, David V J, *et al*. 2004. Parameter estimation of the stochastic AMR model and its application to the study of several strong earthquakes [J]. *Acta Seismologica Sinica*, **17**(2): 177~189.

WANG Wei and LIU Zhen-hua. 1987. Statistical distribution of interval time and abnormal change of seismic risk parameter *D* value before strong earthquakes in North China [J]. *Acta Seismologica Sinica*, **9**(2): 113~127 (in Chinese).

WANG Wei, DAI Wei-le, HUANG Bing-shu. 1994. Statistical distribution of earthquake magnitude and the anomalous change of earthquake magnitude factor *Mf* value before mid—strong earthquakes occurred in North China [J]. *Earthquake Research in China*, **10**(3): 96~110 (in Chinese with English abstract).

WANG Wei DAI Wei-le, SONG Jun-gao. 1999a. The mid-term anomaly variation in spatial scanning of seismic concentrative degree *C*-value before moderate or strong earthquakes in North China [J]. *Earthquake Research*, **22**(1): 51~56 (in Chinese with English abstract).

WANG Wei, SONG Xian-yue, LIU Zheng, *et al*. 1999b. Seismicity factor *A*-value and its application to midterm earthquake prediction in North China [J]. *Earthquake Research in China*, **15**(1): 35~45 (in Chinese with English abstract).

Wyss M and Wiemer S. 1999. How can one test the seismic gap hypothesis?—The case of a repeated ruptures in the Aleutians [J]. *Pure Appl Geophys*, **155**: 259~278.

YIN Xiang-chu and YIN Can. 1991. Instability precursor of nonlinear System and earthquake prediction [J]. *Science in China* (Series B), (5): 512~518 (in Chinese).

YIN Xiang-chu, CHEN Xue-zhong, SONG Zhi-ping, *et al*. 1994. The load-unload response ratio theory: a new approach to earthquake prediction [J]. *Chinese J Geophys*, **37**(6): 764~775 (in Chinese).

ZHANG Zhao-cheng. 1988. *Earthquake Cases in China* (1966~1975) [M]. Beijing: Seismological Press, 1~40, 57~76, 98~116, 155~176, 189~210 (in Chinese).

ZHANG Zhao-cheng. 1990. *Earthquake Cases in China* (1976~1980) [M]. Beijing: Seismological Press, 29~132 (in Chinese).

ZHANG Zhi-jian, DAI Hua-guang, CHEN Wen-bin, *et al*. 2001. the Comprehensive research on deformation system of the Yulekengu earthquake in the middle of ALkin [A]. In: LI Ke eds. The paper collection in the meeting of study on magnitude 8 in China and earthquake prevention and disaster reduction [C]. Beijing: Seismological Press, 216~223 (in Chinese).